

# MRI-Based Visualization of the Relaxation Times of Early Somatic Embryos

J. Mikulka<sup>1</sup>, E. Hutova<sup>1</sup>, R. Korinek<sup>2</sup>, P. Marcon<sup>1</sup>, Z. Dokoupil<sup>2</sup>, E. Gescheidtova<sup>1</sup>, L. Havel<sup>3</sup>, K. Bartusek<sup>2</sup>

<sup>1</sup>*Brno University of Technology, Department of Theoretical and Experimental Electrical Engineering, Technicka 3082/12, 612 00 Brno, Czech Republic*

<sup>2</sup>*Institute of Scientific Instruments, Academy of Sciences of the Czech Republic, Kralovopolska 147, 612 64 Brno, Czech Republic*

<sup>3</sup>*Mendel University in Brno, Faculty of Agronomy, Zemedelska 1, 613 00, Brno, Czech Republic.*

The large set of scientific activities supported by MRI includes, among others, the research of water and mineral compounds transported within a plant, the investigation of cellular processes, and the examination of the growth and development of plants. MRI is a method of major importance for the measurement of early somatic embryos (ESE) during cultivation, and in this respect it offers several significant benefits discussed within this paper. We present the following procedures: non-destructive measurement of the volume and content of water during cultivation; exact three-dimensional differentiation between the ESEs and the medium; investigation of the influence of ions and the change of relaxation times during cultivation; and multiparametric segmentation of MR images to differentiate between embryogenic and non-embryogenic cells. An interesting technique consists in two-parameter imaging of the relaxation times of the callus; this method is characterized by tissue changes during cultivation at a microscopic level, which can be monitored non-destructively.

Keywords: Magnetic measurement, imaging, magnetic susceptibility, calculation, microwave frequencies.

## 1. INTRODUCTION

Magnetic resonance imaging (MRI) is a non-invasive tool widely applied to study molecules. The MRI approach is frequently used not only in medicine but also in biological, biochemical, and chemical research. In plant biology, MRI supports several specialized activities, namely the research of water and mineral compounds transported within a plant [1], [2], the determination of plant metabolites [3], [4], the investigation of cellular processes [5], and the examination of the growth and development of plants [6]. MRI is also employed to monitor water changes in early somatic embryos (ESEs) of spruce [7], [8]. Supalková et al. [9] present the results of a twelve-day, multi-instrumental analytical examination of such early somatic embryos treated with cadmium (II) and/or lead (II) ions (50, 250, and 500 microns). In the investigated ESEs, the researchers have used image analysis to estimate the growth, a fluorimetric sensor to detect the viability, and the MRI technique to facilitate non-destructive measurement of the volume. The embryos constitute a unique plant model system applicable for the study of various types of environmental stresses (including metal ions) under well-controlled experimental conditions

[10], [11], [12]. Nedela et al. [13] visualize the plant extracellular matrix in *Abies alba* and *Abies numidica* by means of a non-commercial environmental scanning electron microscope (ESEM); these authors also studied the morphology of cultured ESEs [13], [14].

This paper discusses the use of MRI in somatic embryogenesis to visualize embryogenic and non-embryogenic callus cultures via both MRI relaxometry and multiparametric image segmentation.

## 2. SUBJECT & METHODS

In order to visualize ESE tissues or highlight their differences according to relevant properties, we can effectively use MRI relaxometry ( $T_1$  and  $T_2$ ) and multiparametric image segmentation. For this purpose, several experiments were performed and are described as follows:

### a) Determining the volume of water in tissues

In MRI, the image intensity corresponds to the number of <sup>1</sup>H nuclei in the investigated tissues or, alternatively, to their relaxation properties. As biological tissues contain significant quantities of water (in comparison with

proton contents in other substances, such as sugars or proteins), MRI image intensities characterize the volume of water in the tissues [15]. To verify the MRI-based results, we compared the water volumes in the ESEs by establishing the change of weight after complete desiccation of the samples with the 3D integral of intensity of the proton density-weighted 3D MR image (proton density measurement using a 4.7 T system). All PD images were standardized to the intensity of the substrate of the first sample. In order to facilitate comparison of the MRI-based measurement and the weighting, we normalized the volumes of water obtained from both measurements according to the volume in the first sample.

#### b) Visualizing the tissue and substrate properties

The different properties of the ESEs and the substrate were measured via MRI, using tomographs with field intensities of 4.7 T and 9.4 T. We also measured MR maps of both the  $^1\text{H}$  nuclear spin density and the  $T_1$  and  $T_2$  relaxation times, and we evaluated the mean densities of these parameters in selected regions.

#### c) Monitoring the relaxation time changes during the growth of the tissues

In the course of the growth of the ESEs, MR images were taken (0 to 15 days), and the  $T_1$  and  $T_2$  relaxation times were evaluated in selected regions. For growth monitoring purposes, the samples were photographed from the bottom side of the applied Petri dish and the ESE area on the medium evaluated on the 0<sup>th</sup>, 5<sup>th</sup>, 7<sup>th</sup>, and 11<sup>th</sup> day of cultivation. The actual experiment involved 2 samples of embryogenic cells for the MRI measurement, 2 samples of embryogenic cells for the verification, and 2 samples of non-embryogenic callus cultures.

#### d) Multiparametric image segmentation

In order to differentiate between the callus and the embryogenic cultures in a sample of non-embryogenic callus cultures, a multiparametric image segmentation method was applied; it utilizes a machine learning algorithm to segment an image according to the distribution of the  $T_2$  relaxation time and the derived images.

To measure the  $T_2$  relaxation (using a 4.7 T system), we applied the spin echo (SE) method ( $T_E = 18, 30, 50, 100,$  and  $200$  ms); the measurement of the  $T_1$  relaxation was performed via inversion recovery (IR) acquisition ( $T_1 = 10, 100, 300, 1000,$  and  $3000$  ms). The  $T_1$  and  $T_2$  relaxations were measured, using a 9.4 T system, by means of the Rapid Acquisition with Refocusing Echoes (RARE) method ( $T_E = 9.8, 29.5, 49.1, 68.8, 88.5, 108.1, 127.8,$  and  $147.4$  ms;  $T_R = 167, 284, 416, 568,$  and  $748$  ms). All the described experiments were carried out on the 4.7 T (Magnex) and 9.4 T (Bruker) MRI systems operated by the Institute of Scientific Instruments, Brno. The MAREVISI (8.2) and MATLAB (7.11.0) programs were used for the actual processing.

### 3. PLANT MATERIAL AND CULTIVATION CONDITIONS

Our experiments involved a clone of early somatic embryos of the Norway spruce (*Picea abies*/L./Karst.) marked as 2/32 and a clone of the Blue spruce (*Picea pungens* Engelm.)

designated as PE 14. The cultures were maintained on a semisolid (Gelrite Gellan Gum, Merck, Germany), half-strength LP medium [16] with modifications [17]. The concentration of 2,4-dichlorophenoxyacetic acid and N<sup>6</sup>-benzyladenine was 4.4 and 9  $\mu\text{M}$ , respectively [18]. The pH value was adjusted to 5.7 - 5.8 before autoclaving (121°C, 100 kPa, 20 min). The organic part of the medium, excluding saccharose, was sterilized by filtering through a 0.2  $\mu\text{m}$  polyethylenesulfone membrane (Whatman, Puradisc 25 AS). The embryos were cultivated in Petri dishes (50 mm in diameter). The sub-cultivation of stock cultures was performed in two-week intervals; the stock and experimental cultures were maintained at the temperature of  $23 \pm 2^\circ\text{C}$  in a cultivation box kept in a dark place.

## 4. RESULTS

### Experiment a)

The experiment started with colonies of ESEs whose weight was about 3 mg; we cultivated ten colonies per one Petri dish. After 2 weeks, the colonies were harvested and, following fresh weight determination, dried to a stable weight at 105°C. In all, thirty-nine colonies were used for the weighting and statistical analysis. A comparison of the volumes of water in the embryos measured via the above-discussed methods can be seen in Fig.1. and Fig.2. While the measurement via desiccation and subsequent weighting was conducted at Mendel University in Brno (MENDELU), the proton density measurement with the SE technique utilized the 4.7 T (Magnex) MRI systems operated by the Institute of Scientific Instruments (ISI), Brno.

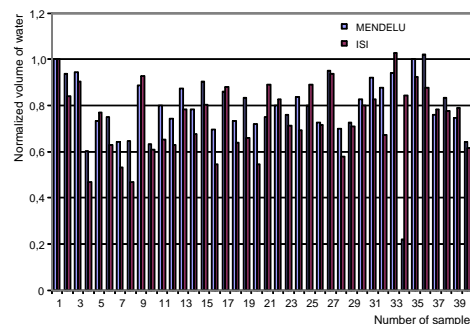


Fig.1. Comparison of the normalized values of samples 1 - 39 measured at the ISI and MENDELU.

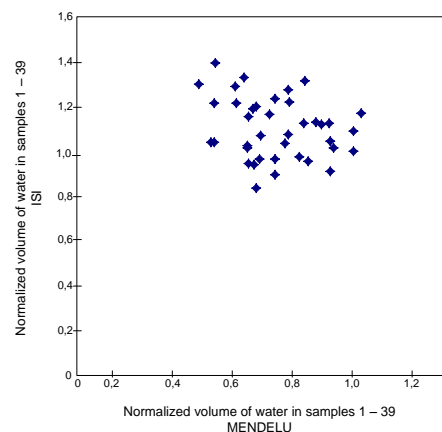


Fig.2. Normalized values of the samples measured at the ISI and MENDELU.

### Experiment b)

After cultivating the two samples for seven days, we measured the proton density (PD) and  $T_1$  and  $T_2$  maps of the ESEs using the 4.7 T and 9.4 T MRI systems. An example of the results obtained with the 9.4 T system is shown in Fig.3.; a comparison of the relaxation times  $T_1$  and  $T_2$  in the embryos and the substrate can be seen in Table 1.

Table 1. Relaxation times  $T_1$  and  $T_2$  in the ESEs and the substrate (sample No. 1).

	$B_0$	$T_1$	$T_2$
	T	ms	ms
<b>ESEs</b>	4.7	622	90
	9.4	1540	85
<b>Substrate</b>	4.7	270	65
	9.4	988	51

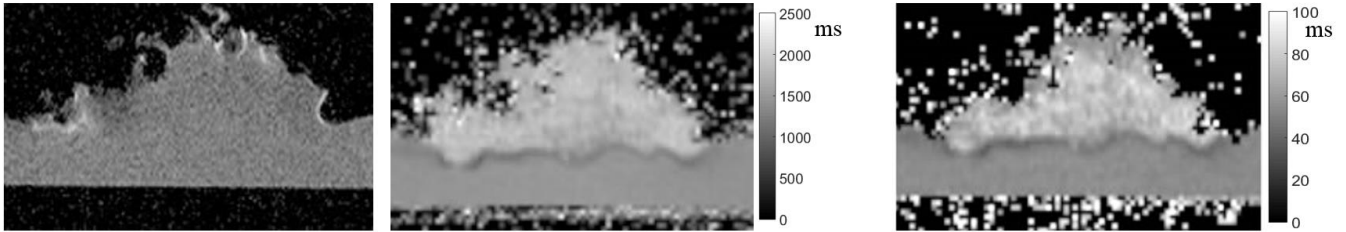


Fig.3. Images of the ESEs (256×256 px; slice thickness of 2 mm) measured with the 9.4 T magnet. Left: PD image; center: the  $T_1$  map; right: the  $T_2$  map.

### Experiment c)

The aim of the experiment was to monitor changes of the ESE area and the relaxation times during the growth phases. To observe the pace of growth in the embryos, we used six Petri dishes, each having 55 mm in diameter and containing a single cluster of ESEs. Photographs (from the bottom side) of a reference sample taken on the 0<sup>th</sup> and 11<sup>th</sup> day of cultivation are shown in Fig.4. The growth of all the samples was monitored according to the size of the ESE area on the medium, Fig.5. In two of the samples, we measured PD weighted,  $T_1$  map and  $T_2$  map MR images, and we also evaluated changes of the relaxation times during the growth phases (Fig.7. and Fig.8.). MR images were not measured in two control samples. Another two, slow-growing samples contained non-embryogenic callus cultures; in these items, we performed an MRI measurement and multiparametric segmentation of the acquired images, and ESE maps with various relaxation properties were created.

with a suitably selected threshold level and for calculating the area of the culture.

As the initial areas of the ESE clusters were not identical, in each area we expressed the percentage of the increase of its original size on the 0<sup>th</sup> day cultivation. The ESE area increase in percent is presented in Fig.5.

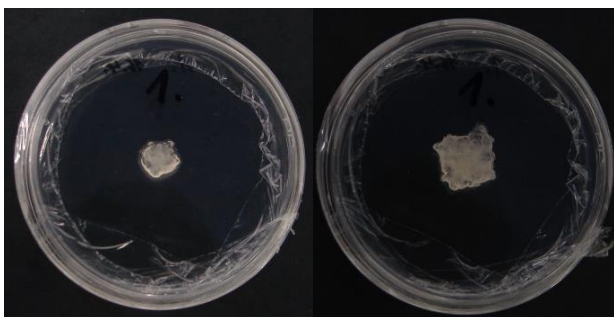


Fig.4. Photographs of an embryonic sample taken on the 0<sup>th</sup> (left) and 11<sup>th</sup> days (right) of cultivation.

The image photographed from the bottom side of the sample (Fig.4.) was used as the basis for segmenting an ESE

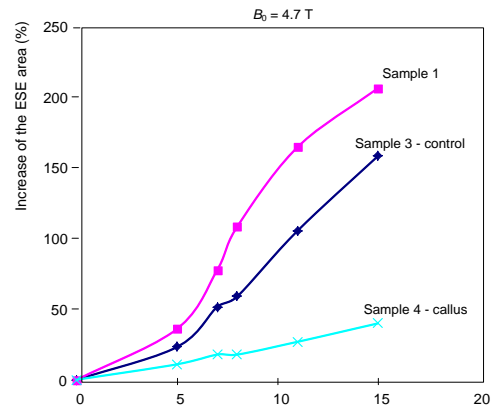


Fig.5. Increase of the ESE area in percent based on the length of the cultivation period.

From the MR images (4.7 T; 256×256 px; layer thickness of 2 mm;  $T_E = 16$  ms;  $T_R = 7000$  ms; and  $T_1 = 10 \div 2000$  ms), the relaxation times  $T_1$  and  $T_2$  and their changes during cultivation were evaluated. Fig.6. below presents MR images weighted by proton density (PD) and the relaxation times  $T_1$  and  $T_2$ . The image intensities were standardized to the intensity of the substrate. The image subregions selected for evaluation were as follows: one subregion in the substrate, two in the culture, and one at the transition between the substrate and the culture. In all these subregions, we evaluated the mean values of  $T_1$  and  $T_2$ ; the obtained results are shown in Fig.7. and Fig.8.

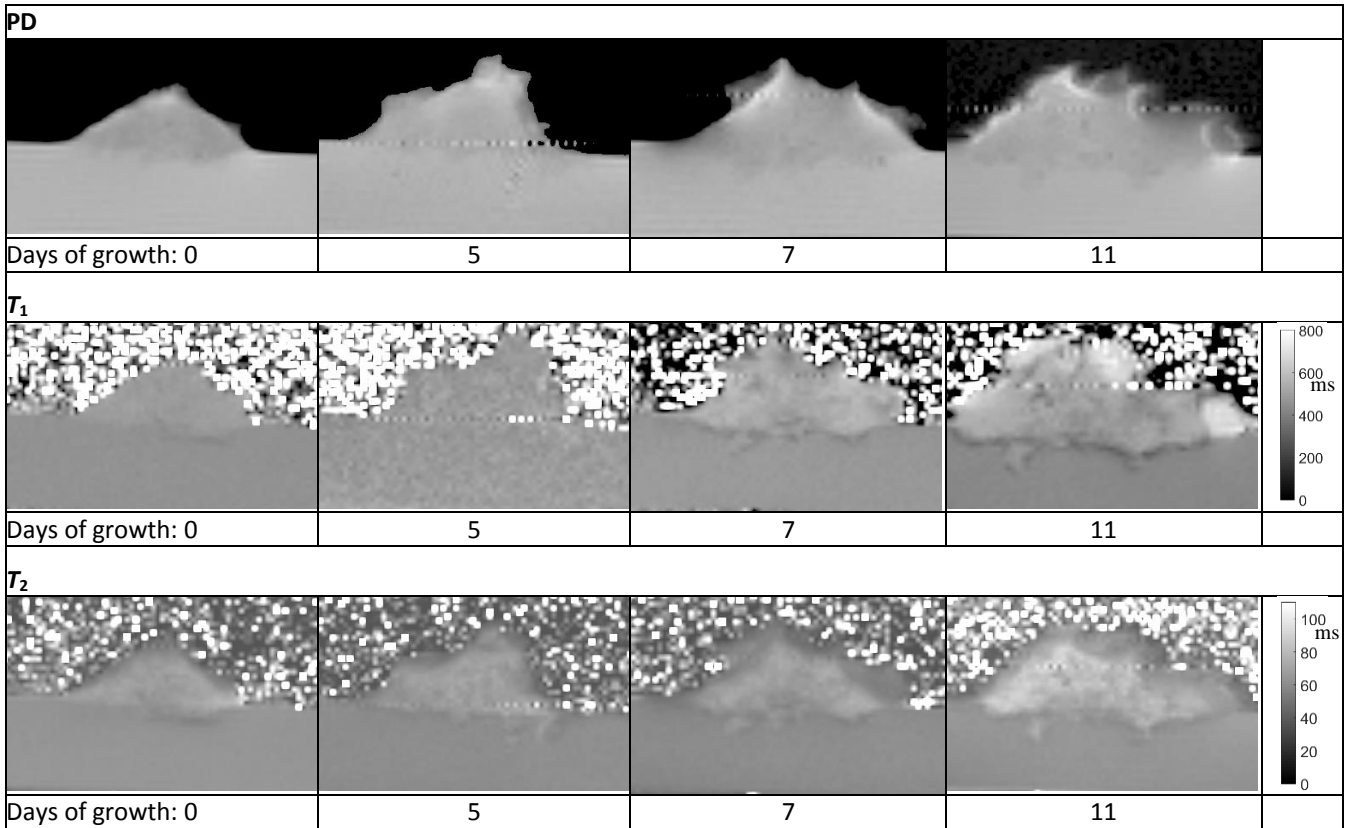


Fig.6. Proton density weighted,  $T_1$  map, and  $T_2$  map ESE images measured during the growth.

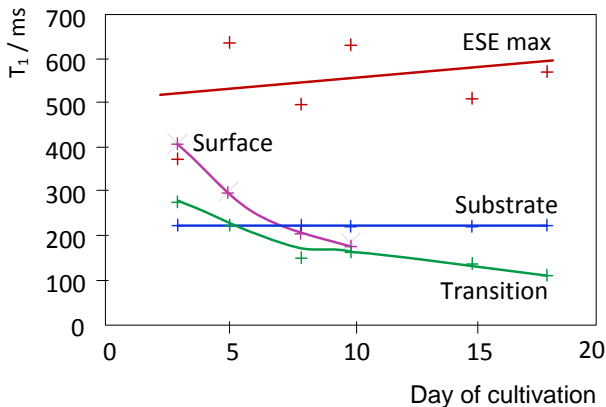


Fig.7. Changes of the relaxation time  $T_1$  in relation to the cultivation time.

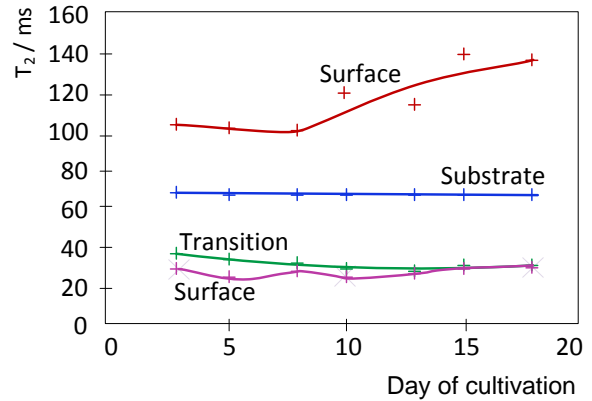


Fig.8. Changes of the relaxation time  $T_2$  in relation to the cultivation time.

**Experiment d)**

While monitoring the tissue growth, we used the available 9.4 T tomograph to acquire MR images. The related field of view (FOV) was 30×30 mm; the 256×256 pixel images exhibit the spatial resolution of 0.117/mm/pixel and slice thickness of 2 mm. The image analysis aimed at differentiating between cells of the callus and the embryogenic culture, and two methods were developed to facilitate this purpose. Generally, the discrimination procedure utilizes machine learning techniques and is hereafter referred to as ML. The aim of the processing is to

segment regions of the tissue culture into two subregions according to the distribution of the relaxation times of the subregions [19]. The measured data were processed in MAREVISI (8.2), MATLAB (7.11.0), and Fiji/ImageJ (1.49) with the Trainable Weka Segmentation plugin. Fig.9. displays the acquired images in the 6<sup>th</sup> slice weighted by proton density and the relaxation times  $T_1$  and  $T_2$  before segmentation. In the following sections of the article, we characterize the ML method, which enabled us to differentiate between the callus and the embryogenic culture in the MR images.



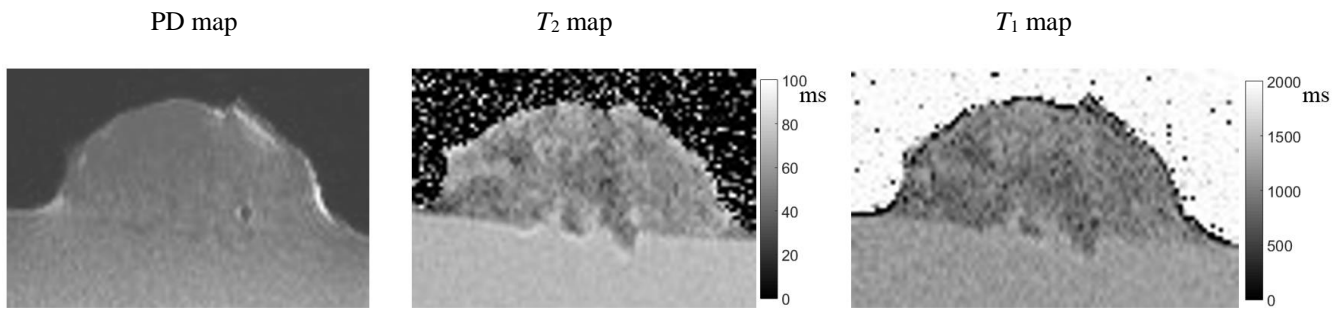


Fig.9. MR images of the non-embryogenic callus cultures.

The **ML method** (Machine Learning) is based on multiparametric classification of MR images [20]. In this technique, the input image is an image weighted by the relaxation time  $T_2$ , and it also consists in images derived from the  $T_2$  map image via pre-processing. More precisely, the relevant image parameters are as follows:

- Image acquired through filtering the original  $T_2$  image by means of a Gaussian filter;
- Hessian of the  $T_2$  image;
- Dispersion of the intensities in the local surroundings of the original  $T_2$  image;
- Minimum intensity in the local surroundings of the original  $T_2$  image;
- Median of the intensities in the local surroundings of the original  $T_2$  image;
- Image obtained through filtering with a bilateral filter.

In total, 7 input images (the original  $T_2$  image and six variants thereof formed via pre-processing) were entered into the applied Random Forest classifier. The discrimination between two subregions in the tissue culture region was carried out with a supervised learning algorithm. A partial result of segmentation performed with the proposed semi-automatic method [21] is shown in Fig.10.; this figure presents images where the intensity of individual pixels expresses the probability with which a given pixel falls within one of the two classification groups. For binary classification of the pixels into the two groups, however, the probabilistic image has to be further processed, and this purpose was advantageously achieved via simple thresholding with threshold choice at 50 % of the maximum intensity of the probabilistic image. The thresholding yields a binary image, namely the result of complete segmentation indicated in the right section of Fig.11.

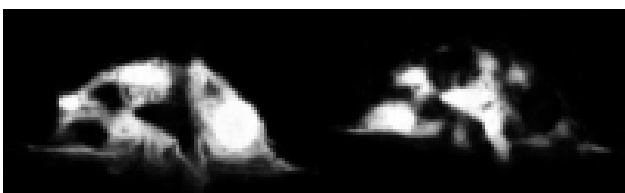


Fig.10. Probabilistic images of the non-embryogenic callus cultures scanned by the 9.4 T tomograph.

The ML-based segmentation of the tissue culture images was performed using the ImageJ/Fiji software with the Trainable Weka Segmentation plugin, which utilizes a very broad package of WEKA (Waikato Environment for Knowledge Analysis) classifiers designed for data mining in Java [22].

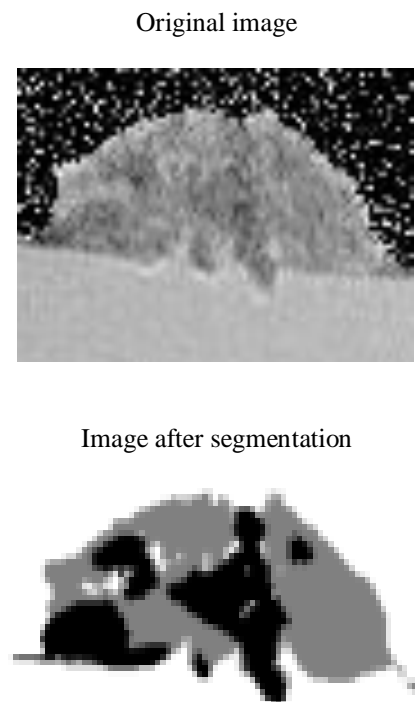


Fig.11. Original  $T_2$  image of the non-embryogenic callus cultures, and classification of the tissue image according to the relaxation time  $T_2$  after segmentation.

## 5. DISCUSSION

In the initial section of the paper, we stated that, in plant biology, MRI supports four basic specialized activities. These are as follows: first, the research of the water and mineral compounds transported within a plant [1], [2]; second, the determination of plant metabolites [3], [4]; third, the investigation of cellular processes [5]; and fourth, the examination of the growth and development of plants [6].

The embryos constitute a unique plant model system applicable for the study of various types of environmental stresses (including metal ions) under well - controlled

experimental conditions [9], [10], [11], [12]. In the investigated ESEs, the researchers have used image analysis to estimate the growth, a fluorimetric sensor to detect the viability, and the MRI technique to facilitate non-destructive measurement of the volume. Pilot studies using two-parameter relaxometry to distinguish between individual areas ESE cultures were performed only at the home institutes of the authors [7], [8].

#### Experiment a)

We utilized two diverse methods to compare the volumes of water in early somatic embryos. While the former technique consists in MRI-based proton density (PD) measurement of the sample, the latter one requires double weighting of the embryos before and after desiccation. The difference in weight is equal to the volume of water in the embryos. The correlation coefficient between the normalized results measured via both methods was 0.816; the results after normalization of the mean value of the determined volumes shown in Fig.1. and Fig.2. exhibit differences. Importantly, the differences between the volumes are caused by several factors: a) evaluation of the volume of water for the inappropriate area affecting the substrate (nutrient medium); b) low sensitivity of the RF coil; c) imperfect image segmentation. With the latter method, the removal of an embryo from the substrate can be accompanied by accidental withdrawal of an amount of material larger than necessary for the subsequent desiccation and weighing. In general, MRI may be used as an effective approach to non-invasive measurement of water in organic structures.

#### Experiment b)

Table 1. shows the relaxation times  $T_1$  and  $T_2$  of the samples in different basic magnetic fields of MR tomographs. The use of a higher magnetic field in combination with a small, high-sensitivity RF coil can improve the signal-to-noise ratio (SNR) and, consequently, provide higher resolution and thinner slices.

At this point, let us note that the volume of water does not change in the individual layers, not even in the transition one; this fact is obvious from the PD images in Fig.3., Fig.6., and Fig.9.

#### Experiment c)

The growth of an ESE area on the medium is presented in Fig.5. Based on the results of the research performed at MENDELU, such growth is proportional to the increase in the volume of the ESEs. The perceptual area growth of non-embryogenic callus cultures corresponds to 40 % in 15 days and is therefore significantly smaller than in the embryogenic ESEs, assuming both the reference samples (158 %) and those measured on the MR tomographs (205 %). The discussed method can be effectively used to monitor the pace of growth of the ESEs.

During such growth, there occur changes of the relaxation times, which correspond to changes in both the chemical composition of the cultures and arrangement of the molecules and their mutual bonds; the said changes of the relaxation

times in the course of cultivation are represented in Fig.7. and Fig.8.

The relaxation time  $T_1$  in the medium does not vary during the growth of the ESEs. On the surface of the culture and on the transition between an ESE and its medium,  $T_1$  is reduced by more than a half in fifteen days, meaning that the chemical structure and arrangement of cells in the given areas are subject to changes during the growth. In the ESEs, the relaxation time  $T_1$  does not change during the growth. Major differences in  $T_1$  are caused by its large inhomogeneity, which probably arises from diverse relaxation properties of the embryonic cells and intercellular mucilage. As regards the growth period of the ESEs, the relaxation time  $T_2$  of the culture does not change for 8 days but then slowly increases from 100 ms up to 140 ms; such behavior may characterize variations of properties of the ESEs, which occur after approximately 8 days. The relaxation time  $T_2$  does not change in the medium, on the surface of the culture or on the transition between the ESEs and the medium, and the cell properties do not vary.

The MR images of the ESEs exhibit large dispersion of the relaxation times ( $T_1$  – 425 to 538 ms;  $T_2$  – 42.6 to 65.6 ms). The inhomogeneity of the relaxation times in the culture points to diverse growth properties of the cells. It is probable that the intraembryonic space contains mucilage, which comprises nutrients in addition to water. Each pixel, having the dimension of 0.117/mm, holds a mixture of the ESEs and mucilage exhibiting a variable volume proportion; this fact then constitutes the cause of large dispersion of the relaxation times.

An important precondition for any 3D measurement of the volume or quantity of water in the ESEs consists in exact identification of the transition layer between the medium and the ESEs. Although this layer is virtually unrecognizable in proton density weighted images, it becomes more perceptible in  $T_1$  map and  $T_2$  map images (Fig.9.). The values in Table 1. show that the relaxation times of the actual transition layer between an ESE and its medium are lower than those in the vicinity of the culture ( $T_1$  by 30 % and  $T_2$  by 22.2 %). During the growth, the transition layer thickness remains very small, amounting to approximately 3 pixels. Generally, changes of the relaxation times, chemical composition of the transition layer, and influence of this layer on the growth of the culture will be subject to further investigation.

#### Experiment d)

A method for the related MR image segmentation was designed and applied. As the traditional, single-parameter approaches fail to function properly in noise-laden MR images with very low contrast, the technique proposed herein is based on an analysis of multiple parameters. In the presented method (ML), the image parameters are created from the original  $T_2$  image, thus forming a vector of 7 features, which suffices for the segmentation of the callus and the embryogenic culture. The segmentation result is indicated in Fig.11. Moreover, the result shows that an MR image can be divided into two regions via automatic processing and, importantly, that such a procedure enables us to differentiate between biologically diverse structures.

## 6. CONCLUSION

Magnetic resonance imaging constitutes a method of major interest for the measurement of ESEs during cultivation, mainly because it offers several significant benefits. These are as follows:

- The technique facilitates non-destructive measurement of the volume and content of water during cultivation, and this procedure is advantageously used in “Multi-instrumental Investigation of Affecting of Early Somatic Embryos of Spruce by Cadmium(II) and Lead(II) Ions” [7];
- The markedly diverse relaxation times  $T_1$  and  $T_2$  provide for exact three-dimensional differentiation between the ESEs and the medium. The chemical composition and properties of the transition layer will be further investigated to define the influence of the said layer on the growth of the cultures;
- The MRI image intensities are proportional to the quantity of  $^1\text{H}$  nuclei in ESEs and to the quantity of water in the tissues;
- Chemical and physical variations in the ESEs affect the growth of the cultures and induce changes of the relaxation times  $T_1$  and  $T_2$  during cultivation; these relaxation time changes then enable non-destructive investigation of the influence of ions (such as Cd, Fe, and Pb) on the ESE cultivation process [7];
- Multiparametric segmentation of MR images may facilitate non-destructive differentiation between embryogenic and non-embryogenic cells in a cultivated culture.

The disadvantages of MRI in monitoring ESEs during their cultivation can be summarized in the following manner:

- Low resolution (less than 0.1 mm) compared to optical or electron microscopy;
- Low sensitivity of the method.

This paper describes non-destructive visualization of embryogenic and non-embryogenic callus cultures using both MRI relaxometry and multiparametric image segmentation. In the given context, an interesting technique consists in two-parameter imaging of the relaxation times  $T_1$  and  $T_2$  of the callus (Fig.4.); its significance consists in the fact that the method is characterized by tissue changes during cultivation at a microscopic level, and said changes can be monitored non-destructively during the entire cultivation period.

## ACKNOWLEDGEMENTS

This work was supported by grant of Ministry of Education, Youth and Sports of the Czech Republic (LO1212) and the project GA 13-09086S.

## REFERENCES

- [1] Schneen, T.W.J., Vergeldt, F.J., Heemskerk, A.M., Van As, H. (2007). Intact plant magnetic resonance imaging to study dynamics in long-distance sap flow and flow-conducting surface area. *Plant Physiology*, 144 (2), 1157-1165.
- [2] Ionenko, I.F., Dautova, N.R., Anisimov, A.V. (2010). Early changes of water diffusional transfer in maize roots under the influence of water stress. *Environmental and Experimental Botany*, 76, 16-23.
- [3] Pu, Y.Q., Chen, F., Ziebell, A., Davison, B.H., Ragauskas, A.J. (2009). NMR characterization of C3H and HCT down-regulated alfalfa lignin. *BioEnergy Research*, 2 (4), 198-208.
- [4] Zulak, K.G., Weljie, A.M., Vogel, H.J., Facchini, P.J. (2008). Quantitative  $^1\text{H}$  NMR metabolomics reveals extensive metabolic reprogramming of primary and secondary metabolism in elicitor-treated opium poppy cell cultures. *BMC Plant Biology*, 8, 5.
- [5] Lambert, J., Lampen, P., von Bohlen, A., Hergenroder, R. (2006). Two- and three-dimensional mapping of the iron distribution in the apoplastic fluid of plant leaf tissue by means of magnetic resonance imaging. *Analytical and Bioanalytical Chemistry*, 384 (1), 231-236.
- [6] Glidewell, S.M., Moller, M., Duncan, G., Mill, R.R., Masson, D., Williamson, B. (2002). NMR imaging as a tool for noninvasive taxonomy: Comparison of female cones of two Podocarpaceae. *New Phytologist*, 154 (1), 197-207.
- [7] Hutová, E., Korinek, R., Bartusek, K., Havel, L. (2013). Comparison and display of the water contained in early somatic embryos. In *PIERS Proceedings*, 12-15 August 2013, Stockholm, Sweden. PIERS, 1671-1674.
- [8] Korinek, R., Havel, L., Hutová, E., Bartusek, K. (2013). MRI contrast in the examination of early somatic embryos. In *Measurement 2013*, 27-30 May 2013. Bratislava, Slovakia: Institute of Measurement Science SAS, 153-156.
- [9] Supalkova, V., Petrek, J., Baloun, J., Adam, V., Bartusek, K., Trnkova, L., Beklova, M., Diopan, V., Havel, L., Kizek, R. (2007). Multi-instrumental investigation of affecting of early somatic embryos of spruce by cadmium(II) and lead(II) ions. *Sensors*, 7 (5), 743-759.
- [10] Mikelova, R., Baloun, J., Petrlova, J., Adam, V., Havel, L., Petrek, H., Horna, A., Kizek, R. (2007). Electrochemical determination of Ag-ions in environment waters and their action on plant embryos. *Bioelectrochemistry*, 70 (2), 508-518.
- [11] Petrek, J., Vitecek, J., Vlasinova, H., Kizek, R., Kramer, K.J., Adam, V., Klejdus, B., Havel, L. (2005). Application of computer imaging, stripping voltammetry and mass spectrometry to study the effect of lead (Pb-EDTA) on the growth and viability of early somatic embryos of Norway spruce (*Picea abies* /L./ Karst.). *Analytical and Bioanalytical Chemistry*, 383 (4), 576-586.
- [12] Viteček, J., Adam, V., Petrek, J., Vacek, J., Kizek, R., Havel, L. (2004). Esterases as a marker for growth of

- BY-2 tobacco cells and early somatic embryos of the Norway spruce. *Plant Cell, Tissue and Organ Culture*, 79 (2), 195-201.
- [13] Nedela, V., Hrib, J., Vookova, B. (2012). Imaging of early conifer embryogenic tissues with the environmental scanning electron microscope. *Biologia Plantarum*, 56 (3), 595-598.
- [14] Nedela, V., Hrib, J., Havel, L., Runstuk, J. (2013). Early state of spruce somatic embryos in native state observed using the ESEM and Cryo-SEM. *Microscopy and Microanalysis*, 19 (S2), 20-21.
- [15] Gruwel, M.L.H., Latta, P., Sbotto-Frankestein, U., Gervai, P. (2013). Visualization of water transport pathways in plants using diffusion tensor imaging. *Progress in Electromagnetic Research C*, 35, 73-82.
- [16] von Arnold, S.J. (1987). Improved efficiency of somatic embryogenesis in mature embryos of *Picea abies* (L.). *Journal of Plant Physiology*, 128, 233-244.
- [17] Havel, L., Durzan, D.J. (1996). Apoptosis during diploid parthenogenesis and early somatic embryogenesis of Norway spruce. *International Journal of Plant Sciences*, 157 (1), 8-16.
- [18] Vlasinova, H., Mikulecky, M., Havel, L. (2003). The mitotic activity of Norway spruce polyembryonic culture oscillates during the synodic lunar cycle. *Biologia Plantarum*, 47 (3), 475-476.
- [19] Mikulka, J., Burget, R., Riha, K., Gescheidtová, E. Segmentation of brain tumor parts in magnetic resonance images. In *36th International Conference on Telecommunications and Signal Processing*, 2-4 July 2013. IEEE, 565-568.
- [20] Dvorak, P., Bartusek, K., Smekal, Z. (2014). Unsupervised pathological area extraction using 3D T2 and FLAIR MR images. *Measurement Science Review*, 14 (6), 357-364.
- [21] Dvorak, P., Kropatsch, W., Bartusek, K. (2013). Automatic brain tumor detection in T2-weighted magnetic resonance images. *Measurement Science Review*, 13 (5), 223-230.
- [22] Hall, M., Frank, E., Holmes, H., Pfahringer, B., Reutemann, P., Witten, I. (2009). The WEKA data mining software: An update. *ACM SIGKDD Explorations Newsletter*, 11 (1), 10-18.

Received December 28, 2015.

Accepted March 22, 2016.